ARPN Journal of Engineering and Applied Sciences

www.arpnjournals.com

A WIDE BANDWIDTH ELEMENT OF SOLAR REFLECT ARRAY ANTENNA WITH SCANNING ABILITY

A. Selamat[1], M. Ramli[1], N. Misran[1], M. F. Mansor[1] and S. H. Zaidi[2]
[1]Centre of Advanced Electronic and Communication Engineering, Faculty of Engineering and Built Environment, Universiti Kebangsaan Malaysia, Malaysia
[2]Solar Energy Research Institute (SERI), Universiti Kebangsaan Malaysia, Malaysia
E-Mail: shade_350@yahoo.com

ABSTARCT

A simple solar cell integrated with a triangular loop shape element of reflects array antenna is presented in this paper. The triangular loop shape element is varied in size to get the required phase range and bandwidth. A wide bandwidth range over 15% has been achieved. Furthermore, a 3 x 3 element reflect array is then formed with 20° scattering angle. A prototype of the solar reflects array cell was fabricated and measured. The measured results show good agreement with simulation. The element is designed to be operated at *Ku*-band frequency and formed a solar reflect array antenna used for terrestrial applications.

Keywords: bandwidth, scattering angle, reflectarray, triangular loop, solar cell.

INTRODUCTION

The reflectarray antenna has long been invented since 1960s [1]. Possessing many advantages such as low manufacturing cost, light weight, flat reflector surface, and easy to deploy have made the antenna preserve to be studied. In addition, the flat reflector surface has the ability to be integrated with solar panel [2]. Although the reflectarray antenna has a potential to replace the conventional parabolic dish antenna, but this sophisticated technology of antenna contributes some limitations due to its narrow bandwidth. The narrow bandwidth corresponds to the differential spatial phase delay of array elements. Element with larger phase range has been demonstrated to improve antenna bandwidth [3]. Therefore, broader phase range has to be achieved in order to improve bandwidth.

Several studies have been carried out to overcome this limitation. The studies included the use of delay lines [4], slotted ground plane [5], the use of a multi-layered substrate [3], [6], etc. Recently, an optimization process has been employed in some studies and bandwidths over 14% have been reported [7-9]. A study involving element with parasitic bipolar has been proved to produce bandwidth of 14.1% [7]. The main dipole element was flanked by the parasitic bipolar to produce broadband reflectarray antenna. In addition, bandwidth of 15.2% has been achieved by [8] using I-shaped element. Each element was tuned to match the required phase delay to obtain a fixed phase difference between two adjacent elements in the optimized band. Furthermore, the use of single layer with multi-resonance element also has been reported to produce bandwidth reaches 17% [9]. The introduction of triple-square-rings element to the reflectarray antenna caused the element's properties to resemble a capacitor and was capable of producing varies phase variation to generate broadband antenna.

In this paper, a simple triangular loop shape element with varied size is presented. A wide bandwidth of 17.5% is achieved by altering the element size. Furthermore, the designed antenna also capable of changing its scattering angle [10]. A prototype of the solar reflectarray antenna has been fabricated and measured. The results for both simulated and measured output are discussed and presented.

ELEMENT DESIGN

The configuration of the single element structure is shown in Figure-1. It is composed of many layers of material to form a solar antenna. The layers comprise of copper on top and bottom of the element structure, a silicon layer, a glass layer, and a Kapton film. The copper on top of the Kapton film was shaped into a triangular loop and works at dual frequencies within *Ku*-band. Detailed dimensions of the triangular loop element can be seen in Table-1. In addition, the glass and silicon layers were formed to be a solar part. Monocrystalline is the selected type of semiconductor for the silicon layer. Once exposed to the sunlight, the *p-n* junction of the monocrystalline is in an 'ON' state condition thus generates electric current.

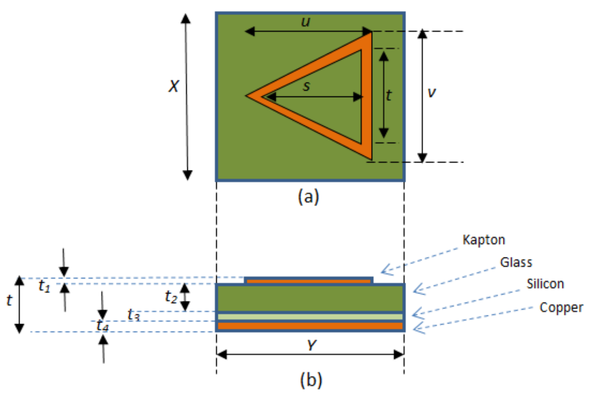

Figure-1. Element structure (a) top view, (b) side view (length X = length Y).

ISSN 1819-6608

Table-1. Dimension of element

Element/ Dimension	***s*** (mm)	***t*** (mm)	***u*** (mm)	***v*** (mm)
Triangular Loop	6.6	6	8	8

Triangular loop element with varied sizes

Phasing scheme of the triangular loop shape element has been set using element of varied sizes. The triangular loop element is altered according to 1: 1 ratio for each side. The ratio is based on the length of '*u*'. The side length of '*u*' is varied from 4.8 mm to 9.6 mm. The changes made to the length '*u*' will also change the dimension size of the triangular loop element. The changes apply to the size of the triangular loop element only and keep everything else constant as in Table-2.

Table-2. Dimension of each layer

Layer / Dimension	***X*** (mm)	***Y*** (mm)	**Thickness** (mm)
Periodicity	10	10	$t = 4.351$
Kapton film	-	-	$t_1 = 0.151$
Silica glass	10	10	$t_2 = 3.900$
Silicon Solar Cell	10	10	$t_3 = 0.200$
Copper (ground)	10	10	$t_4 = 0.100$

CST Microwave Studio software was used to design and simulate the structure. Figure-2 shows the phase response of the triangular element simulated with normal incident plane wave. It is observed that the change in resonant frequency is noticeable starting from 13.2 GHz to 18 GHz in line with changes in length of '*u*' ranging from 4.8 mm to 9.6 mm. The situation occurs due to the modification made in the dimensions of element which in turn changes the surface current flow on the element.

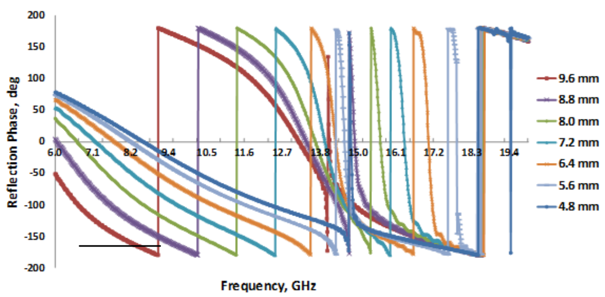

Figure-2. Reflection phase response at different length of '*u*'.

Current distribution of each element also has been observed. Figure-3 shows the current distribution on some selected surface of triangular loop element. It is found that when the length '*u*' was set to 6.4 mm, the surface current marked 60.9 A/m where the element worked at both 14.3 GHz and 16.9 GHz frequencies. But when the length was increased to 8.0 mm, the surface current is reaching the maximum level and marked 209 A/m which operated at 13.7 GHz and 15.5 GHz. It is observed that when the triangular loop element is changing in term of surface size, the resonant frequency is also changing. This feature causes a phase change to the element and further impact the reflectarray antenna phase range and bandwidth. The bandwidth can be measured based on the diagram as depicted in Figure-4 by using equation (1). Referred to Figure-2, element with side length '*u*' set to 8.0 mm has the widest bandwidth which achieved 17.5%. The marked bandwidth is better compared to the bandwidth achieved by [8] and [9].

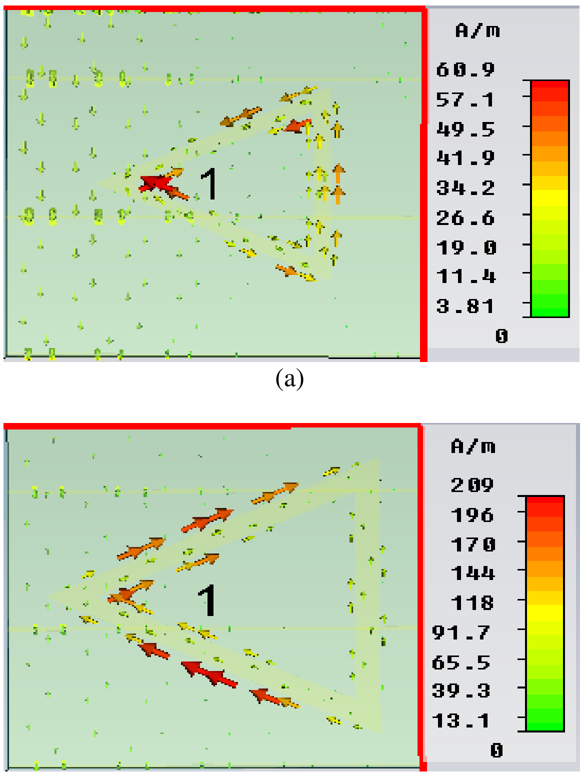

Figure-3. Surface current distribution
(a) u = 6.4 mm, (b) u = 8 mm.

VOL. 13, NO. 24, DECEMBER 2018 ISSN 1819-6608
ARPN Journal of Engineering and Applied Sciences

www.arpnjournals.com

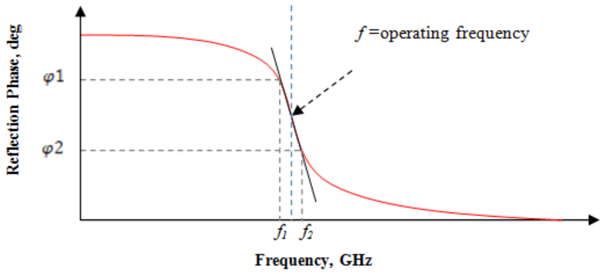

Figure-4. Bandwidth measurement.

$$\text{Bandwidth} = \frac{f_2 - f_1}{f} . (100\%) \quad (1)$$

Meanwhile, a linear phase range performance of the element has also been studied. Figure-5 shows the linear phase range graph obtained from the designed element which operates at 13.7 GHz frequency. The graph is formed by the data obtained from different phases occurred due to the changes in size of the triangular loop element as discussed earlier. The linear phase range is observed to achieve 326°.

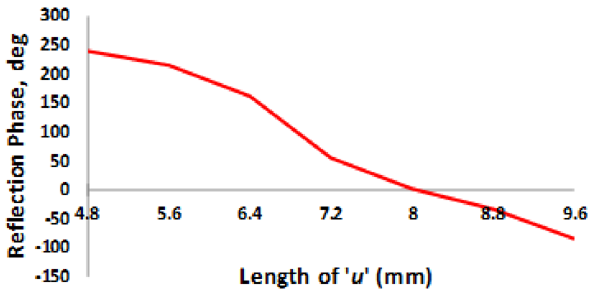

Figure-5. Simulated reflection phase with respect to different lenght of '*u*' at 13.7 GHz.

Furthermore, a result of scattered phase as a function of frequency at different angle of incidence (θ) is simulated and depicted in Figure-6. It is observed that the phase distributions from five different incidence angles between 0° and 50° preserved its original shape. This test is crucial to ensure the designed unit cell can operate at any given radiated beam and work at any given location on antenna surface.

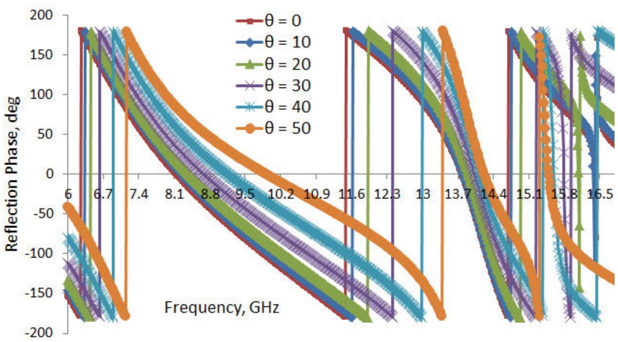

Figure-6. Simulated reflection phase with respect to different lenght of '*u*' at 13.7 GHz.

A 3 x 3 arrays with 20° scattering angle

An additional task has been made to prove that the design element is correct and able to work as an element of reflectarray antenna. The reflectarray element should be able to reflect any incoming signal at any direction according to its unique operating frequency. A 3 x 3 arrays comprising of triangular loop element of different sizes has been designed based on performance graph in Figure-2. The required progressive phase shift (2) between elements is determined to get desired scattered angle [11]. Where λ is the free space wavelength, d the element spacing, and θ the scan angle (scattered angle).

The array has been design so that the incoming signal is scattered at 20°. The complete 3 x 3 arrays diagram is shown in Figure-7. Results from the simulation process have been tabulated as depicted in Figure-8. It is observed that the incident signal has been reflected at the angle of 17° with antenna gain of 8.5 dB. Although the achieved scattered angle was decreased by 3° but this small reduction is considered acceptable.

$$\text{Progressive phase shift} = \frac{2\pi}{\lambda} * d * \sin\theta \quad (2)$$

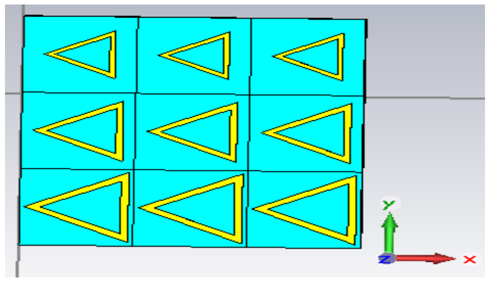

Figure-7. A 3 x 3 arrays designed using CST

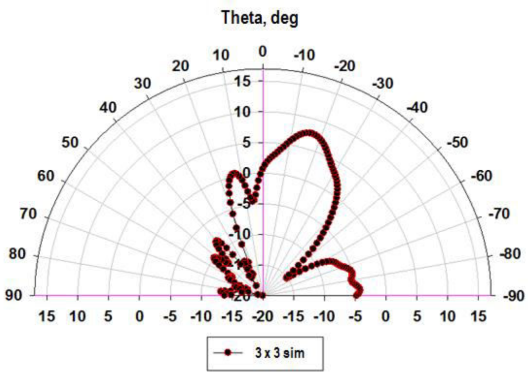

Figure-8. Scattering performance of 3 x 3 arrays

VALIDATION

A prototype of 3 × 3 arrays of triangular loop element is fabricated to form a reflectarray antenna. The reflectarray antenna is designed to operate at *Ku*-band (13.7 GHz) with a scattering angle of 20°. Geometry of the design is shown in Figure-9. The prototype was then measured and evaluated in an anechoic chamber to validate its performance as depicted in Figure-10.

ARPN Journal of Engineering and Applied Sciences

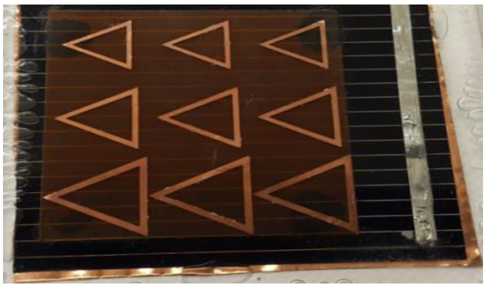

Figure-9. A prototype of 3 x 3 arrays.

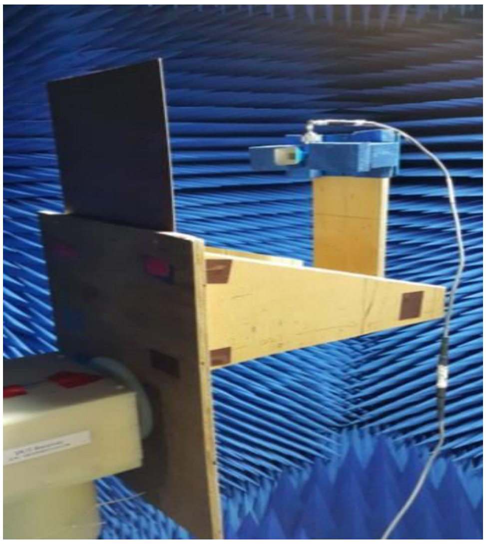

Figure-10. Antenna under test is measured in an anechoic chamber

Figure-11 shows the simulated and measured results of the proposed reflectarray antenna. It is observed that the scattering angles for both methods are in good agreement. The measured results show that the antenna has directed the signal towards 22°. The angle different between both methods is about 5°. From the achieved results, it also can be said that the measurement performance is better compared to simulation as the scattering angle achieved by this method is closer by 2°. Furthermore, the achieved results have been compared with the previous work done by other researchers as shown in Table-3.

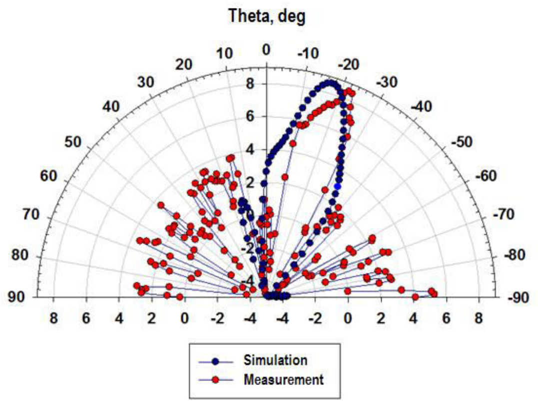

Figure-11. Comparison of scattering performance between simulation and measurement.

Table-3. Comparison with various reflectarray element designs.

Parameter / Design	Design 1 [8]	Design 2 [9]	Proposed design
Element design	Circular ring with I-shaped dipole	Multi-resonance square-ring	Triangular loop with variable size
Bandwidth	15.2%	17%	17.5%
Phase range	More than 360°	More than 360°	326°
Frequency band	*X*-band	K_u-band	K_u-band
Scattering angle	30°	25°	22°
Number of elements	60 elements	480 elements	9 elements
Antenna Gain	15.5 dB	30.8 dB	8.5 dB

CONCLUSIONS

A simple 3 x 3 arrays of triangular loop elements to form a solar reflectarray antenna has been designed. It has been shown that by altering the triangular loop element size has increased the bandwidth over 17%. It is also demonstrated that the 3 x 3 designed arrays able to change its scattering direction of about 22°. Moreover, the measurement results have validated the simulation results.

ACKNOWLEDGEMENT

This work was funded by Universiti Kebangsaan Malaysia under grant no. DIP-2015-014.

REFERENCES

[1] D.G. Berry, R.G. Malech, and W.A. Kennedy. 1963. The reflectarray antenna. IEEE Trans. Antennas Propagat. AP-11: 645-651.

[2] M. Zawadzki and J. Huang. 2000. Integrated RF antenna and solar array for spacecraft applications in Proc. IEEE Int. Conf. On Phased Array Syst. And Techn. pp. 239-242.

[3] J.A. Encinar and J.A. Zornoza. 2003. Broadband design of three-layer printed reflectarrays, IEEE Trans. Antennas Propag. 51(7).

[4] E. Carrasco, M. Barba and J. A. Encinar. 2006. Aperture-coupled reflectarray element with wide range of phase delay, Electron. Lett. 42(12): 667-668.

[5] S. W. Oh, C. H. Ahn and K. Chang. 2009. Reflectarray element using variable ring with slot on ground plane, Electron. Lett. 45(24): 1206-1207.

[6] N. Misran, R. Cahill and V.F. Fusco. 2003. Concentric split ring element for dual frequency reflectarray antennas, Electron Lett. 39(25).

[7] L. Li, Q. Chen, Q. Yuan, K. Sawaya, T. Maruyama, T. Furuno and S. Uebayashi. 2009. Novel broadband planar reflectarray with parasitic dipoles for wireless communication applications, IEEE Antennas Wireless Propag. Lett. 8: 881-885.

[8] Q. Y. Chen, S. W. Qu, J. F Li, Q. Chen and M. Y. Xia. 2013. An X-band reflectarray with novel elements and enhanced bandwidth, IEEE Antennas Wireless Propag. Lett. 12: 317-320.

[9] A. Vosoogh, K. Keyghobad, A. Khaleghi and S. Mansouri. 2014. A high-efficiency Ku-band reflectarray antenna using single-layer multiresonance elements, IEEE Antennas Wireless Propag. Lett. 13: 891-894.

[10] M. Ramli, A. Selamat, N. Misran, M. F. Mansor and M. T. Islam. 2016. Design of capacitive integrated reflectarray radiating elements for beam scanning reconfigurabality, Journal of Eng. And Applied Sciences. 11(1): 106-111.

[11] Hajian M., B.J Kuijpers and L.P. Ligthart. 2006. Reflectarray design using capacitive loading on a slotted patch in Proc. First European Conf. on Antenn and Propagation, EuCAP.